The Journal of Immunology

Osteopontin (Eta-1) and Fibroblast Growth Factor-2 Cross-Talk in Angiogenesis

Daria Leali, Patrizia Dell'Era, Helena Stabile, Barbara Sennino, Ann F. Chambers, Antonella Naldini, Silvano Sozzani, Beatrice Nico, Domenico Ribatti and Marco Presta

J Immunol 2003; 171:1085-1093; ;
doi: 10.4049/jimmunol.171.2.1085
http://www.jimmunol.org/content/171/2/1085

The Journal of Immunology is published twice each month by
The American Association of Immunologists, Inc.,
1451 Rockville Pike, Suite 650, Rockville, MD 20852

Print ISSN: 0022-1767 Online ISSN: 1550-6606.

Osteopontin (Eta-1) and Fibroblast Growth Factor-2 Cross-Talk in Angiogenesis[1]

Daria Leali,* Patrizia Dell'Era,* Helena Stabile,* Barbara Sennino,* Ann F. Chambers,† Antonella Naldini,‡ Silvano Sozzani,* Beatrice Nico,§ Domenico Ribatti,§ and Marco Presta[2]*

The cytokine/extracellular matrix protein osteopontin (OPN/Eta-1) is an important component of cellular immunity and inflammation. It also acts as a survival, cell-adhesive, and chemotactic factor for endothelial cells. Here, subtractive suppression hybridization showed that serum-deprived murine aortic endothelial (MAE) cells transfected with the angiogenic fibroblast growth factor-2 (FGF2) overexpress OPN compared with parental cells. This was confirmed by Northern blotting and Western blot analysis of the conditioned media in different clones of endothelial cells overexpressing FGF2 and in endothelial cells treated with the recombinant growth factor. In vivo, FGF2 caused OPN expression in newly formed endothelium of the chick embryo chorioallantoic membrane (CAM) and of murine s.c. Matrigel plug implants. Recombinant OPN (rOPN), the fusion protein GST-OPN, and the deletion mutant GST-ΔRGD-OPN were angiogenic in the CAM assay. Angiogenesis was also triggered by OPN-transfected MAE cells grafted onto the CAM. OPN-driven neovascularization was independent from endothelial $\alpha_v\beta_3$ integrin engagement and was always paralleled by the appearance of a massive mononuclear cell infiltrate. Accordingly, rOPN, GST-OPN, GST-ΔRGD-OPN, and the conditioned medium of OPN-overexpressing MAE cells were chemotactic for isolated human monocytes. Also, rOPN triggered a proangiogenic phenotype in human monocytes by inducing the expression of the angiogenic cytokines TNF-α and IL-8. OPN-mediated recruitment of proangiogenic monocytes may represent a mechanism of amplification of FGF2-induced neovascularization during inflammation, wound healing, and tumor growth. ***The Journal of Immunology*****, 2003, 171: 1085–1093.**

Angiogenesis plays a key role in different physiological and pathological conditions, including embryonic development, wound repair, inflammation, and tumor growth (1). The local, uncontrolled release of angiogenic growth factors and/or alterations of the production of natural angiogenic inhibitors, with a consequent alteration of the angiogenic balance (2), are responsible for the uncontrolled endothelial cell proliferation that takes place during tumor neovascularization and in angiogenesis-dependent diseases such as diabetic retinopathy, psoriasis, and rheumatoid arthritis (3).

Osteopontin (OPN),[3] also known as early T lymphocyte activation-1 (Eta-1), is a phosphorylated acidic RGD-containing glycoprotein (4–6) that binds certain CD44 variants and integrin receptors, including $\alpha_v\beta_3$ (5). OPN exists both as an immobilized extracellular matrix (ECM) component and as a soluble molecule implicated in inflammation, cell-mediated immunity, tissue remodeling, and tumor metastases (5, 7). OPN acts as a cytokine that plays important roles in monocyte/macrophage functions (5, 7). Experiments performed on OPN-null mice implicate OPN in Th1 cell-mediated immunity during infection, autoimmune demyelinating disease, rheumatoid arthritis, wound healing, and bone resorption (8–11). On the other hand, OPN exerts cell-adhesive and chemotactic activities for endothelial cells that are protected from apoptosis via $\alpha_v\beta_3$ integrin-induced NF-κB activation (12). Also, OPN up-regulation occurs in endothelial cells treated with IL-1, INF-γ, glucocorticoids, or vascular endothelial growth factor (VEGF) (13, 14), during angiogenesis in vitro (15), and during endothelium regeneration in balloon-injured artery (16). Thus, experimental evidence suggests that OPN may affect angiogenesis by acting directly on endothelial cells and/or indirectly via mononuclear phagocyte engagement.

Fibroblast growth factor-2 (FGF2) is one of the best-characterized modulators of angiogenesis (17, 18). FGF2 plays an important role in mediating neovascularization during tumor growth, wound healing, inflammation, and atherosclerosis (19). FGF2 is produced by various tumor and normal cell types, including cells involved in inflammation and immunity such as mononuclear phagocytes (20, 21), $CD4^+$ and $CD8^+$ T lymphocytes (22, 23), and endothelial cells (24).

FGF2 is thought to exert its proangiogenic effect on endothelial cells via a paracrine mode consequent to its release by other cells and/or mobilization from proteoglycans of ECM. On the other

*Unit of General Pathology and Immunology, Department of Biomedical Sciences and Biotechnology, University of Brescia, Brescia, Italy; †Department of Oncology, London Regional Cancer Center, London, Ontario, Canada; ‡Department of Physiology; University of Siena, Siena, Italy; and §Department of Human Anatomy and Histology, University of Bari, Bari, Italy

Received for publication December 12, 2002. Accepted for publication May 16, 2003.

The costs of publication of this article were defrayed in part by the payment of page charges. This article must therefore be hereby marked *advertisement* in accordance with 18 U.S.C. Section 1734 solely to indicate this fact.

[1] This work was supported by grants from Fondazione Italiana per la Lotta al Neuroblastoma (to D.R.); Canadian Breast Cancer Research Initiative (no. 12078, to A.F.C.); Ministero dell'Istruzione, dell'Università e della Ricerca (Cofin 2001, to M.P.); Associazione Italiana per la Ricerca sul Cancro, Istituto Superiore di Sanità (AIDS Project); Ministero dell'Istruzione, dell'Università e della Ricerca (FIRB, Cofin 2002, and Centro di Eccellenza IDET); and Consorzio Italiano Biotecnologie (to M.P.).

[2] Address correspondence and reprint requests to Dr. Marco Presta, Unit of General Pathology and Immunology, Department of Biomedical Sciences and Biotechnology, University of Brescia, Viale Europa 11, 25123 Brescia, Italy. E-mail address: presta@med.unibs.it

[3] Abbreviations used in this paper: OPN, osteopontin; CAM, chick embryo chorioallantoic membrane; ECM, extracellular matrix; EGF, epidermal growth factor; FGF2, fibroblast growth factor-2; rFGF2, recombinant 18-kDa FGF2; MAE cells, murine aortic endothelial cells; FGF2-*T*-MAE cells, FGF2-overexpressing MAE cells; MBE cells; murine microvascular brain endothelial cells; rOPN, recombinant OPN; ΔRGD-OPN, RGD deletion OPN mutant; SSH, subtractive suppression hybridization; VEGF, vascular endothelial growth factor.

0022-1767/03/$02.00

hand, FGF2 may also play an autocrine role in endothelium, leading to the deregulation of endothelial cell behavior (25), as observed for Kaposi's sarcoma (26) and hemangiomas (27). Mouse aortic endothelial (MAE) cells express undetectable levels of FGF2 (28). We generated FGF2-overexpressing pZipFGF2 MAE cells by stable transfection of parental MAE cells with a retroviral expression vector harboring a human FGF2 cDNA (25). Transfectants are characterized by transformed morphology, increased saturation density, invasive and morphogenic behavior in three-dimensional gels, and the capacity to induce opportunistic vascular lesions (25, 28). An FGF2-overexpressing subclone (FGF2-*T*-MAE cells) was isolated from these lesions; it retained several of the in vitro properties of pZipFGF2-MAE cells, but showed a higher tumorigenic capacity when reinjected into nude mice (29). Also, various FGF2-up-regulated transcripts encoding for proteins involved in the modulation of cell cycle, differentiation, stress response, and cell adhesion were identified in FGF2-*T*-MAE cells (30).

In the present paper to gain further insight into the molecular mechanism of FGF2-triggered endothelial cell activation, we performed a subtractive suppression hybridization (SSH) analysis on serum-deprived, growth-arrested FGF2-*T*-MAE transfectants and parental MAE cells. Experimental conditions were chosen to minimize possible differences in gene expression profiles related to the different proliferative status of the two cell types. This approach allowed the identification of OPN as a major FGF2-up-regulated transcript in endothelial cells. The in vitro findings were confirmed in vivo where OPN elicits a potent angiogenic response by causing the recruitment of proangiogenic monocytes. Our results demonstrate the cross-talk among angiogenic growth factors and cytokines during angiogenesis and point to OPN up-regulation as a monocyte-mediated mechanism of amplification of growth factor-induced neovascularization.

Materials and Methods

Reagents

Eukaryotic-produced mouse recombinant OPN (rOPN) and neutralizing anti-mouse OPN Ab were obtained from R&D Systems (Minneapolis, MN). Affinity-purified goat polyclonal anti-OPN Ab was purchased from Santa Cruz Biotechnology (Santa Cruz, CA). Rabbit polyclonal anti-phosphoserine Ab was obtained from Chemicon International (Temecula, CA). Mouse OPN and its RGD deletion mutant (ΔRGD-OPN) were expressed in *Escherichia coli* as GST fusion proteins (31). Recombinant 18-kDa FGF2 was purified from transformed *Escherichia coli* as previously described (32). PMA, epidermal growth factor (EGF), and insulin were obtained from Sigma-Aldrich (St. Louis, MO). The 165-aa VEGF isoform ($VEGF_{165}$) was purchased from Calbiochem (San Diego, CA). Recombinant FGF4 was a generous gift from C. Basilico (New York University Medical Center, New York, NY). SCH 221153 and SCH 216687 were obtained from C. Kumar (Schering-Plough Research Institute, Kenilworth, NJ).

Cell cultures

The BALB/c mouse aortic endothelial 22106 cell line (MAE cells) and the microvascular brain endothelial 10027 cell line (microvascular brain endothelial (MBE) cells) were obtained from R. Auerbach (University of Wisconsin, Madison, WI). They were grown in DMEM (Life Technologies, Gaithersburg, MD) added with 10% FCS. FGF2-transfected pZipFGF2-MAE and pZipFGF2-MBE cells were described previously (25, 33). FGF2-*T*-MAE cells represent a highly tumorigenic pZipFGF2-MAE cell subclone (29). The transfectants were grown in DMEM added with 10% FCS in the presence of 500 μg/ml of G418 sulfate antibiotic (Sigma-Aldrich).

Subtractive suppression hybridization

SSH was performed as previously described (30). Briefly, 2×10^8 MAE and FGF2-*T*-MAE cells grown in complete medium were starved for 48 h in serum-free medium and used for poly(A)$^+$ RNA extraction. Forward SSH (subtraction of FGF-*T*-MAE/MAE) and reverse SSH (subtraction of MAE/FGF-*T*-MAE) were performed with 2 μg of poly(A)$^+$ mRNA from the two cell populations. Eleven strongly positive clones, among several differentially expressed clones hybridizing with cDNA from the forward subtracted library, were partially sequenced using DYEnamic Direct Cycle Sequencing kit (Amersham Pharmacia Biotech, Arlington Heights, IL) exploiting the T7 promoter contained in pCRII-Topo vector (Invitrogen, San Diego, CA). Sequences were read with an automated DNA sequencer (PE Applied Biosystems, Foster City, CA) and compared with GenBank.

Murine OPN cDNA cloning and transfection

Two micrograms of poly(A)$^+$ RNA derived from FGF2-*T*-MAE cells were subjected to reverse transcription using a First Strand cDNA synthesis kit (MBI Fermentas) and an 18-mer oligo(dT) primer. To obtain the entire OPN coding sequence, 1/10th of the reaction was subsequently amplified by PCR using the Advantage-HF PCR kit (Clontech, Palo Alto, CA) using primers based on the published murine OPN mRNA sequence (GenBank accession no. J04806): forward, 5′-GTCTTCTGCGGCAGGCATTCTC GG; reverse, 5′-TGAGCAGTTAGTATTCCTGCTT. The PCR product was cloned in pSTBlue-1 vector using the Perfectly Blunt Cloning Kit (Novagen, San Diego, CA) and were introduced in TOP10F′ competent cells (Invitrogen). Two positive colonies were sequenced. They were identical and showed an A→G substitution at position 365 compared with the published sequence, leading to a Gly→Glu substitution at amino acid position 99. Since our sequence (GenBank accession no. AF515708) was identical with that of several established sequence tags present in GenBank, we cloned our OPN cDNA in the eukaryotic expression vector pBABE Puro (34), thus generating the pBABE-OPN/Puro expression vector. MAE cells (2.5×10^3 cells/100-mm plates) were then transfected with Lipofectamine (Life Technologies) containing 10 μg of pBABE-OPN/Puro or the empty vector. After 72 h, puromycin (4 μg/ml; Sigma-Aldrich) was added to cell cultures. Puromycin-resistant clones were tested for OPN expression by RT-PCR and Western blotting of the cell supernatants.

Evaluation of OPN mRNA expression in endothelial cells

Steady state levels of OPN mRNA were evaluated by Northern blotting of poly(A)$^+$ RNAs (5.0 μg/sample) using a murine OPN probe according to previously described procedures (30). In some experiments OPN expression was evaluated by RT-PCR analysis. To this purpose, RNA was extracted (35), and 2.0 μg of total RNA was retrotranscribed with Ready-To-Go You-Prime First Strand Beads (Amersham Pharmacia Biotech). Then, 1/10th of the reaction (2.0 μl) was amplified in a final volume of 25 μl using the primers for murine OPN (forward, 5′-TGTGTCCTCTGAAG AAAAGGATGAC; reverse, 5′-TCTGTGGCATCAGGATACTGTTCA; product size, 350 bp) and murine GAPDH (forward, 5′-CATGGCCTTC CGTGTTCCTAC; reverse, 5′-TTGCTGTGAAGTCGCAGGAG; product size, 176 bp) at a 0.4-μM final concentration in the same test tube. PCR was performed for one cycle at 95°C (1 min) and 18 cycles at 94°C (30 s), 60°C (30 s), and 72°C (30 s). Aliquots (5 μl) were separated on a 2.0% agarose gel and visualized by ethidium bromide staining.

Conditioned medium preparation and Western blot analysis

To assess the levels of OPN protein released by the different cell lines, cell cultures were grown under serum-free conditions for 1–3 days. Conditioned media were collected and clarified by centrifugation. Western blot analysis was performed on 3–10 μg of total protein using polyclonal anti-mouse OPN Abs.

Purification of murine OPN

Purification of OPN released by FGF2-*T*-MAE cells was performed as previously described (36) with minor modifications. Briefly, FGF2-*T*-MAE cells were seeded in 15-cm dishes at 65,000 cells/cm^2. After 24 h cells were washed twice with DMEM and maintained for 72 h in serum-free DMEM. Fourteen liters of conditioned medium harvested from 800 dishes was then precipitated with 70% ammonium sulfate. Pellet (900 mg of total protein) was resuspended in 50 mM MES/NaOH (pH 6.5), dialyzed against 25 mM MES/NaOH (pH 6.5), and loaded onto an SP-Sepharose column. The flow-through was sequentially incubated with 130 mM sodium citrate and 61 mM barium chloride (15 min each). After centrifugation, the pellet was eluted with 10 ml of 200 mM sodium citrate. Then, 2-ml aliquots (~1.0 mg of total protein) were loaded onto a Mono-Q fast protein liquid chromatography column, and OPN was eluted with a 0.1–1.0 M NaCl linear gradient. Fractions were probed for OPN content by Western blotting (40 μl/fraction) and for cell-adhesive capacity (2.5 μl/fraction). Purified OPN (100 μg/ml, corresponding to peak fractions 15–16 of the chromatographic column shown in Fig. 2*A*) was ~85% pure or better, as shown by Coomassie blue staining of the SDS-PAGE gel (Fig. 2*B*). For evaluation of

OPN phosphorylation, 500-ng aliquots of rOPN and purified OPN were immunoprecipitated with anti-OPN Ab and probed with anti-phosphoserine Ab in a Western blot.

Cell adhesion assay

Aliquots (100 μl) of 100 mM $NaHCO_3$, pH 9.6, containing 2.5 μl of the Mono-Q FPLC column fractions were added to polystyrene nontissue culture microtiter plates. After 16 h of incubation at 4°C, wells were washed with cold PBS and overcoated for 1 h at 37°C with 1.0 mg/ml BSA. Next, MAE cells were seeded onto coated wells (25,000 cells/well) for 2 h at 37°C. Then wells were washed with 2 mM EDTA/PBS. Adherent cells were fixed in 3.7% paraformaldehyde/0.1 M sucrose in PBS and stained with methylene blue/Azur II (1/1, v/v). After solubilization in 10% acetic acid (100 μl/well), plates were read with a microplate reader at 595 nm.

Chicken embryo chorioallantoic membrane assay

Gelatin sponges (Gelfoam, Upjohn, Kalamazoo, MI) cut to 1 mm^3 were placed on top of the CAM of fertilized White Leghorn chicken eggs on day 8 of incubation (37). The sponges were loaded with rOPN, GST-OPN, or GST-ΔRGD-OPN dissolved in 3 μl of PBS or with a 3-μl suspension of OPN-transfected MAE cells in PBS (18,000 cells/sponge) (37). Sponges containing vehicle alone or 1 μg of rFGF2 were used as negative and positive controls, respectively. On day 12, blood vessels entering the sponge within the focal plane of the CAM were counted by two observers in a double-blind fashion at ×50 magnification. Next, all CAMs were processed for light microscopy to assess the angiogenic response by a morphometric method of point counting (37). The microvessel density was expressed as the percentage of the total number of intersection points occupied by blood vessels. The planimetric method was also used for the quantitation of the mononuclear cell infiltrate around blood vessels at the boundary between the sponge and the surrounding CAM mesenchyme. In some experiments CAM fragments underneath the sponges were collected 24 h after implantation and snap-frozen in liquid nitrogen. Extracted total RNAs (2.0 μg) were retrotranscribed, and 1/10th of the reaction was analyzed by PCR using the primers for chicken OPN (forward, 5′-AACAGC CGGACTTTCCTGACAT; reverse, 5′-CACCTCAGGGCTGTGAATCTT; product size, 398 bp) and chicken GAPDH (forward, 5′-CTGAAGGGTGGT GCTAAGCGT; reverse, 5′-TCATACCAGGAAACAAGCTTGACG; product size, 610 bp) as described above. PCR was performed for one cycle at 95°C (1 min) and 23 cycles at 94°C (30 s), 64°C (30 s), and 72°C (45 s). Aliquots (5 μl) were separated on a 1.4% agarose gel and were visualized by ethidium bromide staining.

Immunohistochemistry

For OPN immunodetection in the CAM, a three-layer avidin-biotin-immunoperoxidase system was used (38) on deparaffinized 8-μm sections incubated with goat polyclonal anti-OPN Ab. A preimmune rabbit serum replacing the primary Ab served as a negative control. For OPN immunodetection in the FGF2/Matrigel plug (39), FGF2 (1.0 μg/ml) and heparin (100 μg/ml) were mixed with unpolymerized liquid Matrigel at 4°C to a final volume of 400 μl, then injected s.c. into the flank of female C57BL/6 mice, where it quickly polymerized. Matrigel with PBS alone was used as the negative control. Gels were collected after 7 days, and frozen 5-μm sections were processed for OPN immunostaining as described above.

Electron microscopy

CAM fragments were fixed in ovo in 3% phosphate-buffered glutaraldehyde, dehydrated in serial alcohols, postfixed in 1% phosphate-buffered OsO_4, and embedded in Epon 812. Ultrathin sections were cut in a plane perpendicular to the surface of the CAM and were stained with uranyl acetate, followed by lead citrate. Finally, the sections were examined under a Zeiss 9A electron microscope (New York, NY).

Monocyte isolation

Human monocytes were obtained from buffy coats of healthy blood donors by density gradients on Ficoll/Percoll as previously described (40). When indicated, cells were incubated for 4 h in the absence or the presence of 100 nM rOPN in serum-free RPMI. Then conditioned medium was collected and evaluated for its angiogenic activity in the gelatin sponge/CAM assay (3.0 μl/implant). Fresh medium with or without 100 nM rOPN was used as the negative control. In parallel, monocytes were incubated in fresh medium with 100 nM rOPN. After 4 h, total RNA was extracted, and 2.0 μg was retrotranscribed. Then, 1/10th of the reaction was analyzed by PCR using the primers for human IL-8 (forward, 5′-CGATGTCAGTGCATA AAGACA; reverse, 5′-TGAATTCTCAGCCCTCTTCAAAAA; product size, 225 bp), human TNF-α (forward, 5′-GTCTCCTACCAGACCAAGG TCAACC; reverse, 5′-CAAAGTAGACCTGCCCAGACTCG; product size, 205 bp), and human GAPDH (forward, 5′-ACGGATTTGGTCG TATTGGG; reverse, 5′-TGATTTTGGAGGGATCTCGC; product size, 250 bp) as described above in independent test tubes. For IL-8 and GAPDH, PCR was performed for one cycle at 95°C (1 min) and 23 cycles at 94°C (30 s), 58°C (30 s), and 72°C (20 s). For TNF-α, PCR was performed for one cycle at 95°C (1 min) and 23 cycles at 94°C (30 s), 64°C (30 s), and 72°C (23 s). Aliquots (5 μl) were separated on a 2.0% agarose gel and visualized by ethidium bromide staining.

Monocyte migration assay

Monocyte migration was evaluated using a chemotaxis microchamber technique (NeuroProbe, Pleasanton, CA) using uncoated polycarbonate filters (5-μm pore size; NeuroProbe) as previously described (40). Briefly, chemotactic stimuli (either conditioned media or recombinant proteins) were placed in the lower chamber in RPMI medium with 1.0% FCS. Cells (75,000 cells/well) resuspended in the same medium were added in the upper chamber. Then, the chamber was incubated at 37°C in air with 5% $CO_2$for 90 min. At the end of the incubation, filters were removed and stained with Diff-Quik (Baxter, Rome, Italy). Five high power oil immersion fields were counted.

Results

FGF2 overexpression up-regulates the production of biologically active OPN in endothelial cells

The gene expression profile of growth-arrested FGF2-overexpressing FGF2-*T*-MAE cells was compared with that of parental MAE cells by SSH. To this purpose, both cell types were maintained under serum-free conditions for 48 h before poly(A)$^+$ RNA extraction. Several differentially expressed clones were found to be up-regulated in FGF2-*T*-MAE cells. Partial sequencing of 11 strongly positive clones identified murine OPN as the most representative transcript (nine clones), whereas the other two clones were assigned to Moloney leukemia virus long terminal repeat elements harbored by the pZipFGF2 expression vector (our unpublished observations). In agreement with the SSH data, Northern blot analysis of poly(A)$^+$ RNAs and Western blotting of the serum-free conditioned medium confirmed the dramatic increase in the levels of OPN mRNA and protein in FGF-*T*-MAE cells compared with parental cells (Fig. 1). Semiquantitative Western blot

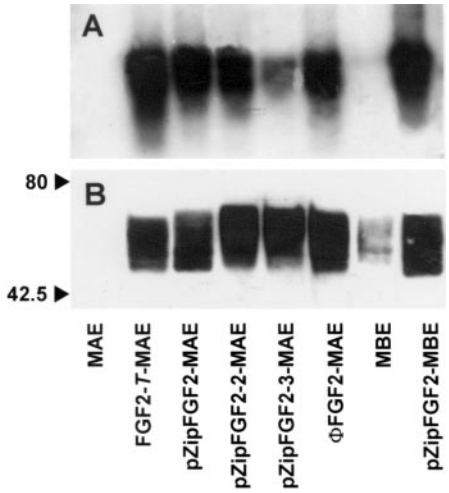

FIGURE 1. OPN up-regulation in FGF2-overexpressing endothelial cells. Parental MAE and MBE cells and their corresponding FGF2 transfectants were grown under serum-free conditions for 48 h. Then, poly(A)$^+$ RNAs (5.0 μg/lane) were probed with a murine OPN probe in a Northern blot (*A*). Uniform loading of the gel was confirmed by rehybridization of the stripped filter with a GAPDH probe (not shown). In parallel, conditioned media (10 μg) were analyzed by Western blotting using affinity-purified polyclonal anti-mouse OPN Abs (*B*).

analysis indicated that FGF2-*T*-MAE cells secrete ~1.0 μg OPN/24 h/10^6 cells. Immunoreactive OPN appeared as a broad band with an apparent molecular mass spanning from ~48 to 65 kDa (Fig. 1*B*) in all the cell lines studied, possibly due to post-translational modifications of the protein (including glycosylation and phosphorylation, see below and Refs. 4–6 and 41).

FGF2-*T*-MAE cells were originated by in vivo selection of FGF2-overexpressing pZipFGF2-MAE cells (29). To confirm that the observed OPN up-regulation does not merely reflect subclonal heterogeneity, OPN expression was investigated in MAE, pZipFGF2-MAE, and FGF2-*T*-MAE cells grown under serum-free conditions, in two independent clones of FGF2-transfected MAE cells (pZipFGF2–2-MAE and pZipFGF2–3-MAE cells), in MAE cells infected with a murine retrovirus harboring the human FGF2 cDNA (ϕFGF2-MAE cells), as well as in parental murine MBE cells and their FGF2-transfected counterpart (pZipFGF2-MBE cells) (25, 33). As shown in Fig. 1, FGF2 overexpression was paralleled by a significant increase in the levels of OPN mRNA and protein in all transfectants.

The OPN/$\alpha_v\beta_3$ integrin interaction mediates endothelial cell adhesion (12), and OPN phosphorylation contributes to integrin binding (42). On this basis, OPN protein was purified from FGF2-*T*-MAE cell-conditioned medium by Mono-Q FPLC chromatography (Fig. 2, *A* and *B*). Then chromatographic fractions were tested for the capacity to mediate the adhesion of parental MAE cells to nontissue culture plastic. OPN immunoreactivity and cell adhesive activity coeluted from the column (Fig. 2, *A* and *B*). Neutralizing anti-murine OPN Ab and the selective $\alpha_v\beta_3/\alpha_v\beta_5$ integrin antagonist SCH 221153, but not the inactive analog SCH 216687 (43), fully inhibited the cell adhesive capacity of purified OPN (Fig. 2*C*). Purified OPN also cross-reacted with anti-phosphoserine Abs (Fig. 2*D*).

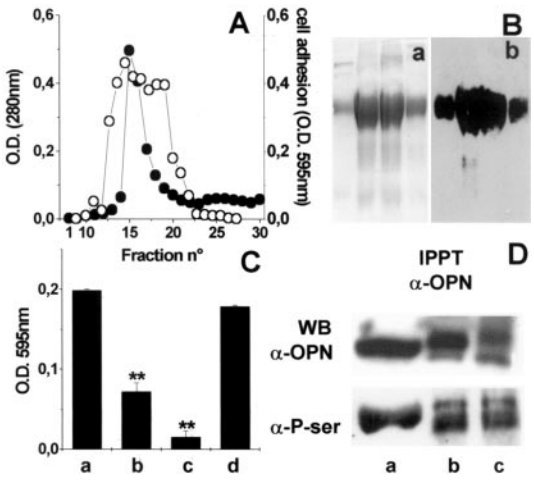

FIGURE 2. Purification of murine OPN. *A*, OPN was purified from the serum-free conditioned medium of FGF2-*T*-MAE cells (see *Materials and Methods*). Mono-Q FPLC fractions (●) were tested (2.5 μl/well) for the capacity to mediate the adhesion of MAE cells to nontissue culture plastic (○). *B*, Ten-microliter aliquots of fractions 14–17 were run on SDS-PAGE. Then total proteins were highlighted by Coomassie blue staining of the gel (*a*) or transferred to a nitrocellulose membrane and probed with anti-OPN Ab in a Western blot (*b*). *C*, Polystyrene nontissue culture microtiter plates were coated with purified OPN (fraction 15). Then, MAE cell adhesion was evaluated in the absence of any competitor (*a*), 10 μg/ml of neutralizing anti-OPN Ab (*b*), 30 μM of the $\alpha_v\beta_3/\alpha_v\beta_5$ integrin antagonist SCH 221153 (*c*), or of the inactive analog SCH 216687 (*d*). Data are the mean ± SD of three determinations (**, $p < 0.01$). *D*, Eukaryotic-produced rOPN (*b*; 500 ng) and purified OPN (*c*) were immunoprecipitated (IPPT) with anti-OPN Ab (α-OPN). Immunoprecipitates (*b* and *c*) and nonimmunoprecipitated rOPN (*a*) were then probed in a Western blot (WB) with the same anti-OPN Ab and with anti-phosphoserine Ab (α-P-ser).

Recombinant FGF2 up-regulates OPN production in endothelial cells

FGF2-overexpressing MAE cells release limited amounts of FGF2 (~100 pg/96 h/10^6 cells) that acts on the same cells via an extracellular mechanism of autocrine stimulation (28). On this basis, we evaluated the capacity of exogenous human recombinant FGF2 (rFGF2) to modulate OPN expression in MAE cells. As illustrated in Fig. 3*A*, rFGF2 increased steady state levels of OPN mRNA, as assessed by semiquantitative RT-PCR analysis. This was followed by a significant production of OPN protein that accumulated in the conditioned medium 6 h after stimulation and reached a plateau at 24 h (Fig. 3*B*).

As shown in Fig. 3*C*, FGF4 was similar to FGF2 in the ability to induce a significant increase in the levels of secreted OPN protein; PMA and EGF were less effective, whereas $VEGF_{165}$ and insulin were ineffective.

Next, we evaluated the effect of rFGF2 on endothelial cell OPN production in vivo. To this purpose, rFGF2 was delivered onto the CAM of the chick embryo via a gelatin sponge implant or was administered s.c. in BALB/c mice via a Matrigel plug, two experimental models widely used to study the proangiogenic activity of FGF2 (39, 44). As shown in Fig. 4*B* (*inset*), rFGF2 causes up-regulation of OPN mRNA expression in the CAM that was paralleled by a significant increase in OPN immunoreactivity of the

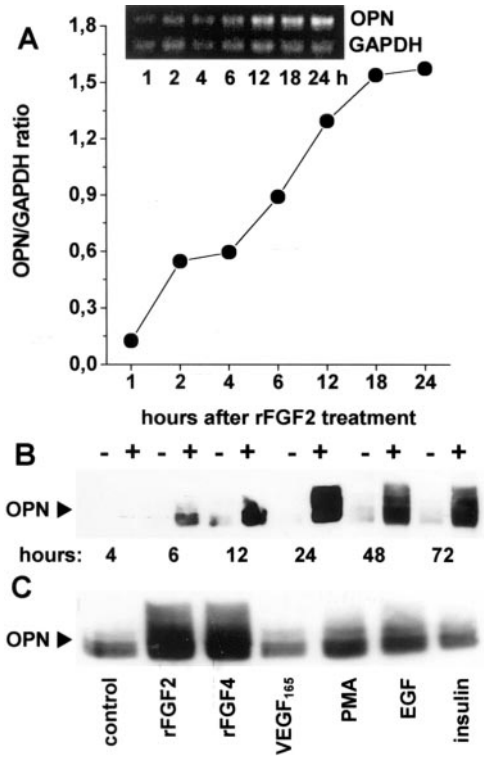

FIGURE 3. Recombinant FGF induces OPN up-regulation in MAE cells. MAE cells were incubated under serum-free conditions with 100 ng/ml of rFGF2. At different time points, RNA was extracted and RT-PCR was performed using specific murine OPN primers. Murine GAPDH primers were used for the loading controls. Data are expressed as the OPN/GAPDH ratio of the intensity of the corresponding PCR bands (*A*). In parallel, conditioned media collected at different time points from control (−) or rFGF2-treated (+) cell cultures were analyzed by Western blotting using affinity-purified anti-mouse OPN Abs (*B*). *C*, Cells were incubated under serum-free conditions for 48 h with the indicated stimuli (all at 100 ng/ml). At the end of incubation, conditioned media were collected and analyzed by Western blotting using affinity-purified polyclonal anti-mouse OPN Abs.

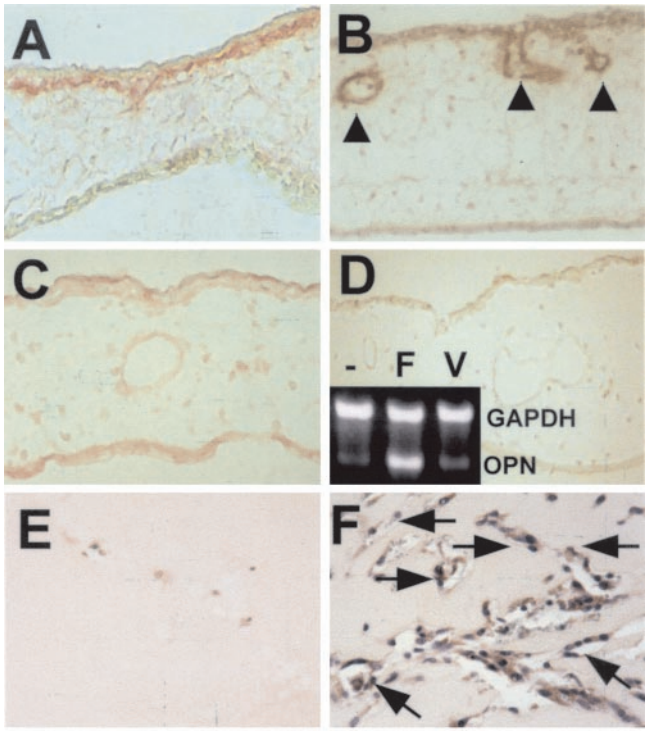

FIGURE 4. Recombinant FGF2 induces endothelial OPN up-regulation in vivo. *A–D*, Gelatin sponges adsorbed with vehicle (*A*), 1.0 μg of rFGF2 (*B* and *D*), or 1.0 μg of $VEGF_{165}$ (*C*) were loaded onto the CAM of 8-day embryos. CAM fragments underneath the gelatin sponges were decorated with affinity-purified goat polyclonal anti-OPN Ab on day 12 or assessed by RT-PCR for OPN expression on day 9. OPN immunoreactivity is evident in newly formed blood vessels (arrowheads) of rFGF2-treated CAMs (*B*) and limited to the basement membrane of the chorionic epithelium and stroma in control (*A*) and $VEGF_{165}$-treated (*C*) CAMs. No specific signal was observed in rFGF2-treated CAMs in which the primary Ab was replaced by preimmune rabbit serum (*D*). RT-PCR for OPN expression was performed using specific chicken OPN primers in CAMs treated with vehicle (−), rFGF2 (*F*), or $VEGF_{165}$ (V; *inset* in *D*). Chicken GAPDH primers were used for the loading controls. *E* and *F*, Control and FGF2/Matrigel plugs were implanted s.c. into the flank of female C57BL/6 mice, After 7 days gels were collected and frozen, and 5-μm sections were processed for OPN immunostaining and nuclear counterstaining. Note the strong OPN signal present in the endothelium lining the numerous blood vessels (arrows) of FGF2/Matrigel plugs (*F*) that were absent in control plugs (*E*). Infiltrating mononuclear cells were also evident in FGF2/Matrigel plugs (*F*).

newly formed endothelium (Fig. 4*B*). No OPN mRNA up-regulation and blood vessel OPN immunoreactivity was instead observed in $VEGF_{165}$-treated CAMs compared with controls (Fig. 4). A strong OPN immunoreactivity was also associated with the newly formed blood vessels infiltrating the rFGF2/Matrigel plugs in mice, which was rarely observed in control plugs (Fig. 4, *E* and *F*).

Proangiogenic activity of OPN

OPN is endowed with endothelial cell adhesive capacity (see above) and represents a chemotactic stimulus for different cell types, including endothelial cells (45). On the other hand, OPN is devoid of any mitogenic activity for endothelial cells (46). Indeed, [^{3}H]thymidine incorporation in serum-deprived MAE cells (754 ± 11 cpm/well) was not affected by eukaryotic-produced murine rOPN administered at doses ranging between 1.0 and 1,000 ng/ml (from 550 ± 155 to 844 ± 80 cpm/well) compared with cells treated with 30 ng/ml rFGF2 (4630 ± 573 cpm/well). Because of the hypothesized direct and/or indirect involvement of OPN in angiogenesis (see introduction), we investigated the impact of rOPN on the developing endothelium of the CAM, an assay widely used to evaluate pro- and antiangiogenic compounds (47). Macroscopic observation showed that rOPN induces a strong angiogenic response in the CAM (Fig. 5*C*), similar to rFGF2 (Fig. 5*A*). No vascular reaction was instead detectable in the embryos treated with PBS (Fig. 5*B*).

Histological quantitation of microvessel density within the gelatin implants confirmed the proangiogenic activity of rOPN (Table I). However, in keeping with the chemotactic activity of OPN for mononuclear phagocytes (7), implants adsorbed with rOPN showed a massive mononuclear cell infiltrate at histological and ultrastructural levels (Fig. 6, *A–E*). Infiltrating mononuclear cells were also observed in rFGF2-treated CAMs, even though at a lower number than in rOPN-treated CAMs, but were rarely seen in control CAMs (Fig. 6 and Table I).

Compared with the application on the CAM of large amounts of recombinant proteins in a single bolus, the use of cell implants overexpressing the corresponding gene allows continuous delivery of the protein when produced by a limited number of cells, thus mimicking more closely the events that may occur in vivo (48). On this basis, MAE cells were transfected with an expression vector harboring the murine OPN cDNA previously cloned from the FGF2-*T*-MAE poly(A)$^+$ RNA population (see *Materials and Methods*). Selected MAE-OPN A4, A6, and B5 transfectants released significant amounts of OPN compared with MAE-V2 and V13 mock cells (Fig. 7*A*, *inset*). No significant differences were observed among the various clones and parental cells in their rates of growth, in agreement with the incapacity of rOPN to stimulate the proliferation of parental MAE cells. Also, OPN overexpression did not confer to MAE cells the capacity to grow in vivo when injected s.c. in nude mice (our unpublished observations).

OPN transfectants exerted a strong angiogenic response when grafted onto the CAM, similar to that exerted by rOPN (Fig. 7*A*). Again, neovascularization was paralleled by a significant increase

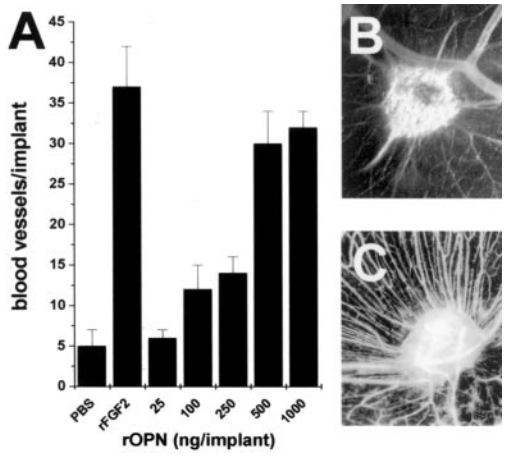

FIGURE 5. Recombinant OPN stimulates angiogenesis in the CAM. Vehicle (PBS), 1 μg of rFGF2, or increasing concentrations of rOPN were delivered onto the CAM. After 4 days, blood vessels entering the implant were counted under a stereomicroscope. Data are the mean ± SD of 10 embryos (*A*). Implant and surrounding CAM specimens were dissected ex ovo and placed on a dark background. Images were then captured with a digital camera using a sidelight. Digitized 24-bit color images were then converted to 8-bit gray scale images, and their contrast was increased by 25% to highlight blood vessels using the Paint Shop Pro software (version 7.00; Jasco, Easton, MD). Note the highly vascularized appearance of rOPN implant (C) compared with the control sponge (B).

Table I. *Effect of rOPN on CAM vascularization*[a]

Treatment	Microvessel Density: Intersection points (mean ± SD)	Microvessel Density: Area (% of total)	Mononuclear Cell Infiltrate: Cells/field (mean ± SD)
PBS	0	0	10 ± 2
rFGF2	30 ± 4[b]	20.8	30 ± 7[b]
rOPN	24 ± 6[b]	16.7	125 ± 2[b]

[a] Gelatin sponges adsorbed with vehicle, rFGF2, or rOPN (both at 1.0 μg/embryo) were implanted onto the CAM of 8-day embryos (10 animals/group). Histological sections of the CAMs were analyzed on day 12 for evaluation of microvessel density and of the mononuclear cell infiltrate around blood vessels at the boundary between the sponge and the surrounding CAM mesenchyme.

[b] $p < 0.01$ vs control (by Student's t test).

in the mononuclear cell infiltrate (Fig. 7*B*). No neoangiogenesis and mononuclear cell infiltrate were observed in the CAMs grafted with parental or mock-transfected MAE cells. Accordingly, the conditioned medium of OPN-overexpressing clones was endowed with a significant chemotactic activity for freshly isolated human monocytes compared with the conditioned medium of mock-transfected and parental cells (Fig. 7*C*).

Angiogenic activity of rOPN is independent of $\alpha_v\beta_3$ integrin interaction

Indirect experimental evidences suggest a role for OPN/$\alpha_v\beta_3$ integrin interaction in angiogenesis (14, 45). To assess this hypothesis we took advantage of the fact that deletion of the RGD sequence in OPN abolishes integrin engagement in endothelial cells (45). Accordingly, MAE cells adhere and spread on plastic coated with a GST-OPN chimera, but not with the GST-ΔRGD-OPN mutant. Also, the GST-ΔRGD-OPN mutant does not appear to exert a significant chemotactic activity for MAE cells (data not shown). On this basis, the GST-ΔRGD-OPN mutant was compared with GST-OPN for its angiogenic capacity in vivo. As shown Fig. 8*A*, the GST-ΔRGD-OPN mutant retains angiogenic activity in the CAM assay analogous to that exerted by GST-OPN and rOPN. Again, a significant mononuclear cell infiltrate was observed in CAMs treated with GST-ΔRGD-OPN or GST-OPN (Fig. 8*B*) that also exerted a chemotactic activity in vitro for human monocytes (Fig. 8*C*). No angiogenic and chemotactic activities were instead exerted by control GST (our unpublished observations). Thus, endothelial $\alpha_v\beta_3$ integrin engagement does not appear to be responsible for the angiogenic response triggered by OPN.

Recombinant OPN induces a proangiogenic phenotype in human monocytes

Monocytes play a important role in angiogenesis (49–51). The mononuclear cell infiltrate constantly observed in OPN-treated CAMs may therefore be responsible, at least in part, for the neovascular response triggered by this cytokine. Indeed, semiquantitative RT-PCR analysis demonstrates that incubation with 100 nM rOPN causes up-regulation of the proangiogenic cytokines TNF-α (52) and IL-8 (53) in freshly isolated human monocytes (Fig. 9, *inset*). Also, an ~2-fold increase in the levels of proangiogenic IL-6 (54) was demonstrated by ELISA in the conditioned medium of rOPN-treated monocytes compared with controls (our unpublished observations). Thus, OPN deeply affects the angiogenic potential of human monocytes. Accordingly, the conditioned medium of rOPN-treated human monocytes induces neovascularization when applied to the CAM (Fig. 9). No significant angiogenic response was elicited by fresh medium added with the same dose of rOPN, corresponding to 18 ng/embryo and therefore 5 times lower than the minimal angiogenic dose (see Fig. 5*A*) or by the conditioned medium of untreated monocytes (Fig. 9). These data point to a role for mononuclear cell infiltrate in mediating the angiogenic activity exerted in vivo by OPN.

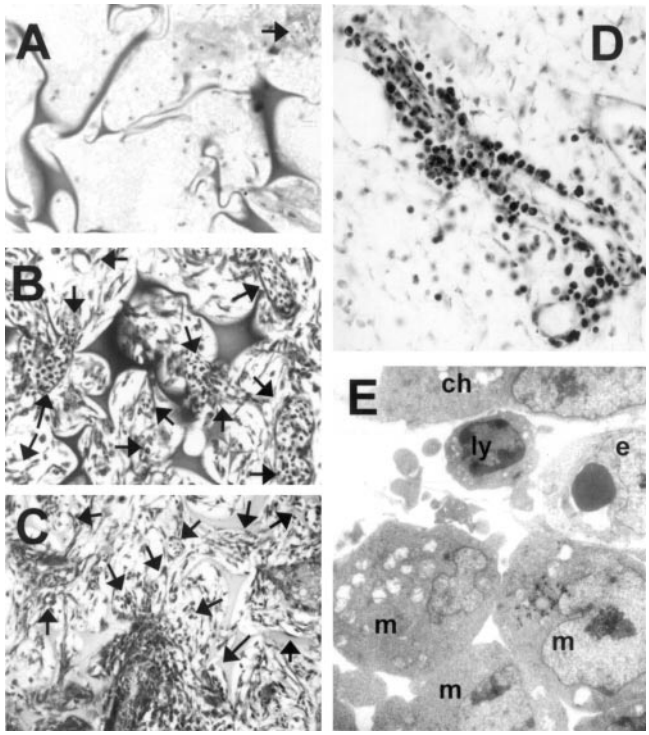

FIGURE 6. Mononuclear cell infiltrate characterizes rOPN-treated CAMs. CAMs were treated as described in Fig. 5. Then, histological sections of gelatin sponge implants were stained with H&E. A collagenous matrix containing numerous capillaries (arrows) and a moderate mononuclear cell infiltrate are present among the trabeculae of rFGF2-treated sponges (*B*). No neovascularization and infiltrate are instead observed in control sponges (*A*). Numerous capillaries (arrows) and an intense mononuclear cell infiltrate are evident in rOPN-treated implants (*C*). Mononuclear cells frequently encircle microvessels located at the boundary between the rOPN-loaded sponges and the surrounding CAM mesenchyme (*D*). *E*, Mononuclear cells (m) and a lymphocyte (ly) are recognizable at ultrastructural level around a capillary (e) beneath the chorionic epithelium (ch) in an rOPN-treated CAM.

Discussion

In the present paper OPN has been identified as an FGF2-up-regulated transcript by SSH performed on quiescent, serum-deprived endothelial FGF2-*T*-MAE cells compared with parental cells. OPN up-regulation was confirmed on various independent FGF2-overexpressing clones originating from murine endothelial cells. The increased OPN production by FGF2 transfectants is possibly due to an extracellular mechanism of action of the released growth factor that interacts with its tyrosine kinase receptors (25, 28). In agreement with this hypothesis, treatment of parental MAE cells with rFGF2 led to a significant increase in OPN production and release, similar to that observed for FGF2 transfectants. OPN up-regulation was also observed in MBE cells, murine microvascular endothelial cells isolated from s.c. implants, and immortalized bovine adrenal gland microvascular endothelial cells treated with rFGF2 (our unpublished observations). In keeping with a receptor-mediated mechanism of action, the tyrosine kinase FGFR inhibitor tyrphostin 23 (55) prevented OPN induction by rFGF2 (our unpublished observations). Additional experiments are required to

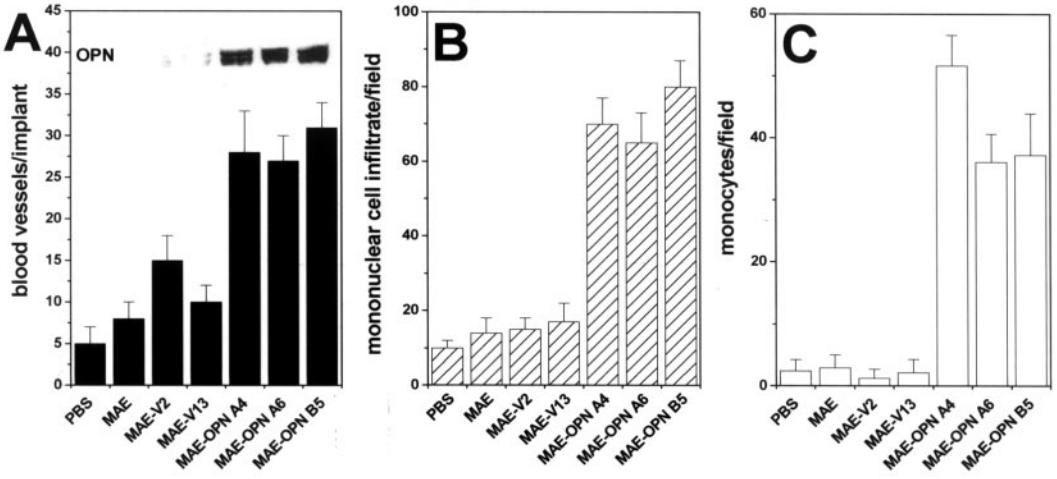

FIGURE 7. Angiogenic activity of OPN-overexpressing MAE cells. Parental, mock-transfected MAE-V2 and MAE-V13, and OPN-transfected MAE-OPN A4, A6, and B5 cells were grafted on the CAM via a gelatin sponge implant (18,000 cells/embryo). On day 12, blood vessels entering the sponge were counted (*A*). Mononuclear cell infiltrate was assessed on histological sections of the CAMs by a planimetric method of point counting (*B*). One-microgram aliquots of serum-free conditioned media of the different cell types were evaluated for their chemotactic activity on freshly isolated human monocytes (*C*), whereas 10-μg aliquots were probed with anti-OPN Ab in a Western blot (*inset* in *A*).

elucidate the role of FGFR signaling in OPN up-regulation by endogenous and exogenous FGF2.

In agreement with the in vitro findings, rFGF2 caused OPN up-regulation in vivo in newly formed blood vessels of the chick embryo CAM and in s.c. murine Matrigel plugs. This extends previous observations about OPN expression by endothelial cells in different pathological conditions (16, 45, 56). Interestingly, we did not observe OPN up-regulation in $VEGF_{165}$-treated CAMs, in keeping with the incapacity of this growth factor to increase OPN production in MAE cells. At variance, VEGF has been shown to increase OPN mRNA expression in human dermal microvascular endothelial cells (14). Endothelial cell heterogeneity may explain this apparent discrepancy.

Up to 28 phosphorylated residues can be present in OPN that are differently induced by phorbol ester and cytokines. Interestingly, phosphorylation may affect receptor binding and biological activity of OPN (see Ref. 41 and references therein). Accordingly, our data indicate that OPN is produced in a phosphorylated, cell-adhesive form by FGF2-overxpressing MAE cells. Immobilized OPN mediates endothelial cell adhesion via $\alpha_v\beta_3$ integrin engagement (45) and favors endothelial cell survival (12). In contrast, soluble OPN does not support endothelial cell survival and is unable to stimulate endothelial cell proliferation (46). Indeed, phosphorylated OPN purified from FGF2-*T*-MAE cell-conditioned medium mediates MAE cell adhesion when immobilized to the substratum, and rOPN does not stimulate MAE cell proliferation when given as a soluble molecule. The lack of mitogenic activity of OPN for endothelial cells is supported further by the lack of effect of OPN overexpression on in vitro and in vivo growth properties of MAE transfectants.

Here we demonstrate that OPN exerts a potent angiogenic activity in vivo despite its inability to stimulate endothelial cell proliferation in vitro. Also, the capacity of GST-ΔRGD-OPN to elicit a full angiogenic response indicates that endothelial $\alpha_v\beta_3$ integrin engagement and cell adhesion are not responsible for the proangiogenic activity of OPN. Even though we cannot rule out the

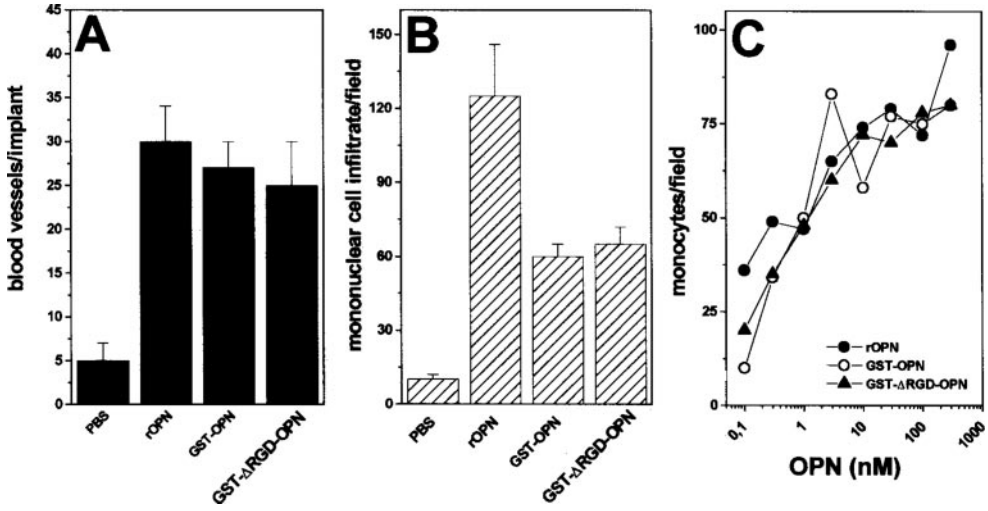

FIGURE 8. Angiogenic activity of ΔRGD-OPN mutant. Gelatin sponges adsorbed with vehicle (PBS), rOPN, GST-OPN, or GST-ΔRGD-OPN (500 ng/implant) were implanted onto the CAM ($n = 10$). After 4 days, blood vessels entering the sponge were counted (*A*). Mononuclear cell infiltrate was assessed on histological sections of the CAMs by a planimetric method of point counting (*B*). Increasing concentrations of rOPN (●), GST-OPN (○), and GST-ΔRGD-OPN (▲) were evaluated for their chemotactic activity on freshly isolated human monocytes (*C*).

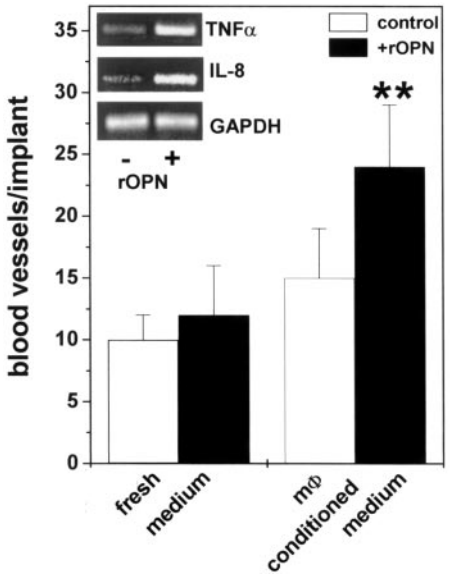

FIGURE 9. Angiogenic activity of OPN-treated human monocytes. Human monocytes (mϕ) were incubated for 48 h in the absence (□) or the presence (■) of 100 nM rOPN in serum-free RPMI. Then conditioned media were evaluated for their angiogenic activity in the CAM (3.0 μl/implant). Fresh medium with or without 100 nM rOPN was used as a negative control. **, $p < 0.01$ vs control. *Inset*, Monocytes were incubated for 4 h in the absence or the presence of 100 nM rOPN. Then RNA was extracted, and RT-PCR was performed using specific human TNF-α and IL-8 primers. Human GAPDH primers were used for the loading controls.

possibility that an integrin-independent interaction(s) with endothelial cells may contribute to OPN-driven neovascularization, our data suggest that the activity of OPN is due at least in part to an indirect mechanism of action consequent to the recruitment of proangiogenic monocytes. Several experimental evidences support this hypothesis.

OPN-induced angiogenesis was always paralleled by the recruitment of a massive mononuclear cell infiltrate. Accordingly, rOPN, GST-OPN, and GST-ΔRGD-OPN induced a chemotactic response on isolated human monocytes. Also, the angiogenic response elicited by OPN-overexpressing MAE cells was paralleled by a significant mononuclear cell infiltrate, and their conditioned medium was chemoattractant for isolated human monocytes. No neovascularization and mononuclear cell infiltrate were observed in CAMs treated with control GST or with parental or mock-transfected MAE cells, thus confirming the specificity of the response. Our data are in keeping with the ability of OPN to cause macrophage recruitment at the site of injection after s.c. administration (57). Also, the capacity of GST-ΔRGD-OPN to exert monocyte chemoattraction in vitro and in vivo indicates that this occurs via an RGD-independent mechanism of action, possibly consequent to OPN/CD44 receptor interaction (58).

Monocyte/macrophage functions are deeply affected by OPN (5, 7). Experiments performed on OPN-null mice implicate OPN in Th1 cell-mediated immunity during infection, autoimmune demyelinating disease, rheumatoid arthritis, wound healing, and bone resorption (8–11). All these conditions are characterized by mononuclear phagocyte involvement and neovascularization that is impaired in OPN null mice (10, 59). Monocytes express a variety of angiogenic growth factors (49–51). Among them, TNF-α plays a pivotal role in mediating macrophage-induced angiogenesis (52). Here, in keeping with a putative role for recruited mononuclear phagocytes in OPN-triggered angiogenesis, rOPN induces the expression of TNF-α as well as of the proangiogenic chemokines IL-8 (53) and IL-6 (54) in human monocytes. Accordingly, the conditioned medium of rOPN-treated monocytes caused a strong angiogenic response in the CAM.

FGF2 induces neovascularization in the CAM and in the murine Matrigel plug assay (37, 39). In both assays endothelium of the newly formed blood vessels cross-reacts with anti-OPN Abs. Also, a mononuclear cell infiltrate is present in the mesoderm of FGF2-treated CAMs compared with controls. The presence of this infiltrate, even though less massive than in OPN-treated CAMs, suggests that the recruitment of proangiogenic monocytes may contribute at least in part to the angiogenic activity of FGF2. This hypothesis is supported by the presence of a mononuclear cell infiltrate also in neovascularized FGF2/Matrigel plugs (see Fig. 4). In keeping with these observations, Abs to either IL-1 or TNF-α can blunt the angiogenic response to FGF2 (49).

In conclusion, our data demonstrate that FGF2 causes OPN up-regulation in endothelial cells in vitro and in vivo. This results in the recruitment of proangiogenic monocytes. OPN up-regulation thus may represent a mechanism of amplification of growth factor-induced neovascularization in different physiopathological conditions, including inflammation, wound healing, and tumor growth.

References

1. Carmeliet, P., and R. K. Jain. 2000. Angiogenesis in cancer and other diseases. *Nature 407:249.*
2. Hanahan, D., and J. Folkman. 1996. Patterns and emerging mechanisms of the angiogenic switch during tumorigenesis. *Cell 86:353.*
3. Folkman, J. 1995. Angiogenesis in cancer, vascular, rheumatoid and other disease. *Nat. Med. 1:27.*
4. Denhardt, D. T., and X. Guo. 1993. Osteopontin: a protein with diverse functions. *FASEB J. 7:1475.*
5. Denhardt, D. T., M. Noda, A. W. O'Regan, D. Pavlin, and J. S. Berman. 2001. Osteopontin as a means to cope with environmental insults: regulation of inflammation, tissue remodeling, and cell survival. *J. Clin. Invest. 107:1055.*
6. Furger, K. A., K. M. Rajashree, A. B. Tuck, V. H. C. Bramwell, and A. F. Chambers. 2001. The functional and clinical roles of osteopontin in cancer and metastasis. *Curr. Mol. Med. 1:621.*
7. O'Regan, A. W., G. J. Nau, G. L. Chupp, and J. S. Berman. 2000. Osteopontin (Eta-1) in cell-mediated immunity: teaching an old dog new tricks. *Immunol. Today 21:475.*
8. Yoshitake, H., S. R. Rittling, D. T. Denhardt, and M. Noda. 1999. Osteopontin-deficient mice are resistant to ovariectomy-induced bone resorption. *Proc. Natl. Acad. Sci. USA 96:8156.*
9. Ashkar, S., G. F. Weber, V. Panoutsakopoulou, M. E. Sanchirico, M. Jansson, S. Zawaideh, S. R. Rittling, D. T. Denhardt, M. J. Glimcher, and H. Cantor. 2000. Eta-1 (osteopontin): an early component of type-1 (cell-mediated) immunity. *Science 287:860.*
10. Yumoto, K., M. Ishijima, S. R. Rittling, K. Tsuji, Y. Tsuchiya, S. Kon, A. Nifuji, T. Uede, D. T. Denhardt, and M. Noda. 2002. Osteopontin deficiency protects joints against destruction in anti-type II collagen antibody-induced arthritis in mice. *Proc. Natl. Acad. Sci. USA 99:4556.*
11. Liaw, L., D. E. Birk, C. B. Ballas, J. S. Whitsitt, J. M. Davidson, and B. L. Hogan. 1998. Altered wound healing in mice lacking a functional osteopontin gene (spp1). *J. Clin. Invest. 101:1468.*
12. Scatena, M., M. Almeida, M. L. Chaisson, N. Fausto, R. F. Nicosia, and C. M. Giachelli. 1998. NF-κB mediates $\alpha_v\beta_3$ integrin-induced endothelial cell survival. *J. Cell Biol. 141:1083.*
13. Singh, K., J. L. Balligand, T. A. Fischer, T. W. Smith, and R. A. Kelly. 1995. Glucocorticoids increase osteopontin expression in cardiac myocytes and microvascular endothelial cells: role in regulation of inducible nitric oxide synthase. *J. Biol. Chem. 270:28471.*
14. Senger, D. R., S. R. Ledbetter, K. P. Claffey, A. Papadopoulos-Sergiou, C. A. Peruzzi, and M. Detmar. 1996. Stimulation of endothelial cell migration by vascular permeability factor/vascular endothelial growth factor through cooperative mechanisms involving the alphavbeta3 integrin, osteopontin, and thrombin. *Am. J. Pathol. 149:293.*
15. Prols, F., B. Loser, and M. Marx. 1998. Differential expression of osteopontin, PC4, and CEC5, a novel mRNA species, during in vitro angiogenesis. *Exp. Cell. Res. 239:1.*
16. O'Brien, E. R., M. R. Garvin, D. K. Stewart, T. Hinohara, J. B. Simpson, S. M. Schwartz, and C. M. Giachelli. 1994. Osteopontin is synthesized by macrophage, smooth muscle, and endothelial cells in primary and restenotic human coronary atherosclerotic plaques. *Arterioscler. Thromb. 14:1648.*
17. Basilico, C., and D. Moscatelli. 1992. The FGF family of growth factors and oncogenes. *Adv. Cancer Res. 59:115.*
18. Javerzat, S., P. Auguste, and A. Bikfalvi. 2002. The role of fibroblast growth factors in vascular development. *Trends Mol. Med. 8:483.*
19. Nugent, M. A., and R. V. Iozzo. 2000. Fibroblast growth factor-2. *Int. J. Biochem. Cell. Biol. 32:115.*

20. Kuwabara, K., S. Ogawa, M. Matsumoto, S. Koga, M. Clauss, D. J. Pinsky, P. Lyn, J. Leavy, L. Witte, J. Joseph-Silverstein, et al. 1995. Hypoxia-mediated induction of acidic/basic fibroblast growth factor and platelet-derived growth factor in mononuclear phagocytes stimulates growth of hypoxic endothelial cells. *Proc. Natl. Acad. Sci. USA 92:4606.*
21. Baird, A., P. Mormede, and P. Bohlen. 1985. Immunoreactive fibroblast growth factor in cells of peritoneal exudate suggests its identity with macrophage-derived growth factor. *Biochim. Biophys. Acta 126:358.*
22. Blotnick, S., G. E. Peoples, M. R. Freeman, T. J. Eberlein, and M. Klagsbrun. 1994. T lymphocytes synthesize and export heparin-binding epidermal growth factor-like growth factor and basic fibroblast growth factor, mitogens for vascular cells and fibroblasts: differential production and release by $CD4^+$ and $CD8^+$ T cells. *Proc. Natl. Acad. Sci. USA 91:2890.*
23. Peoples, G. E., S. Blotnick, K. Takahashi, M. R. Freeman, M. Klagsbrun, and T. J. Eberlein. 1995. T lymphocytes that infiltrate tumors and atherosclerotic plaques produce heparin-binding epidermal growth factor-like growth factor and basic fibroblast growth factor: a potential pathologic role. *Proc. Natl. Acad. Sci. USA 92:6547.*
24. Dell'Era, P., M. Presta, and G. Ragnotti. 1991. Nuclear localization of endogenous basic fibroblast growth factor in cultured endothelial cells. *Exp. Cell. Res. 192:505.*
25. Gualandris, A., M. Rusnati, M. Belleri, E. E. Nelli, M. Bastaki, M. P. Molinari-Tosatti, F. Bonardi, S. Parolini, A. Albini, L. Morbidelli, et al. 1996. Basic fibroblast growth factor overexpression in endothelial cells: an autocrine mechanism for angiogenesis and angioproliferative diseases. *Cell Growth Differ. 7:147.*
26. Ensoli, B., R. Gendelman, P. Markham, V. Fiorelli, S. Colombini, M. Raffeld, A. Cafaro, H. K. Chang, J. N. Brady, and R. C. Gallo. 1994. Synergy between basic fibroblast growth factor and HIV-1 Tat protein in induction of Kaposi's sarcoma. *Nature 371:674.*
27. Takahashi, K., J. B. Mulliken, H. P. Kozakewich, R. A. Rogers, J. Folkman, and R. A. Ezekowitz. 1994. Cellular markers that distinguish the phases of hemangioma during infancy and childhood. *J. Clin. Invest. 93:2357.*
28. Ribatti, D., A. Gualandris, M. Belleri, L. Massardi, B. Nico, M. Rusnati, P. Dell'Era, A. Vacca, L. Roncali, and M. Presta. 1999. Alterations of blood vessel development by endothelial cells overexpressing fibroblast growth factor-2. *J. Pathol. 189:590.*
29. Liekens, S., J. Neyts, E. De Clercq, E. Verbeken, D. Ribatti, and M. Presta. 2001. Inhibition of fibroblast growth factor-2-induced vascular tumor formation by the acyclic nucleoside phosphonate cidofovir. *Cancer Res. 61:5057.*
30. Dell'Era, P., L. Coco, R. Ronca, B. Sennino, and M. Presta. 2002. Gene expression profile in fibroblast growth factor 2-transformed endothelial cells. *Oncogene 21:2433.*
31. Xuan, J. W., C. Hota, Y. Shigeyama, J. A. D'Errico, M. J. Somerman, and A. F. Chambers. 1995. Site-directed mutagenesis of the arginine-glycine-aspartic acid sequence in osteopontin destroys cell adhesion and migration functions. *J. Cell Biochem. 57:680.*
32. Gualandris, A., C. Urbinati, M. Rusnati, M. Ziche, and M. Presta. 1994. Interaction of high-molecular-weight basic fibroblast growth factor with endothelium: biological activity and intracellular fate of human recombinant M(r) 24,000 bFGF. *J. Cell Physiol. 161:149.*
33. Gualandris, A., M. Rusnati, M. Belleri, M. P. Molinari-Tosatti, F. Bonardi, A. Albini, M. Ziche, and M. Presta. 1996. Angiogenic phenotype induced by basic fibroblast growth factor transfection in brain microvascular endothelial cells: an in vitro autocrine model of angiogenesis in brain tumors. *Int. J. Oncol. 8:567.*
34. Morgenstern, J. P., and H. Land. 1990. Advanced mammalian gene transfer: high titre retroviral vectors with multiple drug selection markers and a complementary helper-free packaging cell line. *Nucleic Acids Res. 18:3587.*
35. Chomczynski, P., and N. Sacchi. 1987. Single-step method of RNA isolation by acid guanidinium thiocyanate-phenol-chloroform extraction. *Anal. Biochem. 162:156.*
36. Liaw, L., M. Almeida, C. E. Hart, S. M. Schwartz, and C. M. Giachelli. 1994. Osteopontin promotes vascular cell adhesion and spreading and is chemotactic for smooth muscle cells in vitro. *Circ. Res. 74:214.*
37. Ribatti, D., A. Gualandris, M. Bastaki, A. Vacca, M. Iurlaro, L. Roncali, and M. Presta. 1997. New model for the study of angiogenesis and antiangiogenesis in the chick embryo chorioallantoic membrane: the gelatin sponge/chorioallantoic membrane assay. *J. Vasc. Res. 34:455.*
38. Ribatti, D., B. Nico, A. Vacca, and L. Roncali. 1999. Localization of factor VIII-related antigen in the endothelium of the chick embryo chorioallantoic membrane. *Histochem. Cell. Biol. 112:447.*
39. Passaniti, A., R. M. Taylor, R. Pili, Y. Guo, P. V. Long, J. A. Haney, R. R. Pauly, D. S. Grant, and G. R. Martin. 1992. A simple, quantitative method for assessing angiogenesis and antiangiogenic agents using reconstituted basement membrane, heparin, and fibroblast growth factor. *Lab. Invest. 67:519.*
40. Bonecchi, R., F. Facchetti, S. Dusi, W. Luini, D. Lissandrini, M. Simmelink, M. Locati, S. Bernasconi, P. Allavena, E. Brandt, et al. 2000. Induction of functional IL-8 receptors by IL-4 and IL-13 in human monocytes. *J. Immunol. 164:3862.*
41. Weber, G. F., S. Zawaideh, S. Hikita, V. A. Kumar, H. Cantor, and S. Ashkar. 2002. Phosphorylation-dependent interaction of osteopontin with its receptors regulates macrophage migration and activation. *J. Leukocyte Biol. 72:752.*
42. Ek-Rylander, B., M. Flores, M. Wendel, D. Heinegard, and G. Andersson. 1994. Dephosphorylation of osteopontin and bone sialoprotein by osteoclastic tartrate-resistant acid phosphatase: modulation of osteoclast adhesion in vitro. *J. Biol. Chem. 269:14853.*
43. Kumar, C. C., M. Malkowski, Z. Yin, E. Tanghetti, B. Yaremko, T. Nechuta, J. Varner, M. Liu, E. M. Smith, B. Neustadt, et al. 2001. Inhibition of angiogenesis and tumor growth by SCH221153, a dual $\alpha_v\beta_3$ and $\alpha_v\beta_5$ integrin receptor antagonist. *Cancer Res. 61:2232.*
44. Ribatti, D., B. Nico, A. Vacca, L. Roncali, P. H. Burri, and V. Djonov. 2001. Chorioallantoic membrane capillary bed: a useful target for studying angiogenesis and anti-angiogenesis in vivo. *Anat. Rec. 264:317.*
45. Liaw, L., V. Lindner, S. M. Schwartz, A. F. Chambers, and C. M. Giachelli. 1995. Osteopontin and β_3 integrin are coordinately expressed in regenerating endothelium in vivo and stimulate Arg-Gly-Asp-dependent endothelial migration in vitro. *Circ. Res. 77:665.*
46. Rittling, S. R., Y. Chen, F. Feng, and Y. Wu. 2002. Tumor-derived osteopontin is soluble, not matrix associated. *J. Biol. Chem. 277:9175.*
47. Ribatti, D., A. Vacca, L. Roncali, and F. Dammacco. 2000. The chick embryo chorioallantoic membrane as a model for in vivo research on anti-angiogenesis. *Curr. Pharm. Biotechnol. 1:73.*
48. Ribatti, D., B. Nico, L. Morbidelli, S. Donnini, M. Ziche, A. Vacca, L. Roncali, and M. Presta. 2001. Cell-mediated delivery of fibroblast growth factor-2 and vascular endothelial growth factor onto the chick chorioallantoic membrane: endothelial fenestration and angiogenesis. *J. Vasc. Res. 38:389.*
49. Jackson, J. R., M. P. Seed, C. H. Kircher, D. A. Willoughby, and J. D. Winkler. 1997. The codependence of angiogenesis and chronic inflammation. *FASEB J. 11:457.*
50. Sunderkotter, C., K. Steinbrink, M. Goebeler, R. Bhardwaj, and C. Sorg. 1994. Macrophages and angiogenesis. *J. Leukocyte Biol. 55:410.*
51. Mantovani, A. 1994. Tumor-associated macrophages in neoplastic progression: a paradigm for the in vivo function of chemokines. *Lab. Invest. 71:5.*
52. Leibovich, S. J., P. J. Polverini, H. M. Shepard, D. M. Wiseman, V. Shively, and N. Nuseir. 1987. Macrophage-induced angiogenesis is mediated by tumour necrosis factor-α. *Nature 329:630.*
53. Belperio, J. A., M. P. Keane, D. A. Arenberg, C. L. Addison, J. E. Ehlert, M. D. Burdick, and R. M. Strieter. 2000. CXC chemokines in angiogenesis. *J. Leukocyte Biol. 68:1.*
54. Cohen, T., D. Nahari, L. W. Cerem, G. Neufeld, and B. Z. Levi. 1996. Interleukin 6 induces the expression of vascular endothelial growth factor. *J. Biol. Chem. 271:736.*
55. Boyer, B., and J. P. Thiery. 1993. Cyclic AMP distinguishes between two functions of acidic FGF in a rat bladder carcinoma cell line. *J. Cell Biol. 120:767.*
56. Shijubo, N., T. Uede, S. Kon, M. Maeda, T. Segawa, A. Imada, M. Hirasawa, and S. Abe. 1999. Vascular endothelial growth factor and osteopontin in stage I lung adenocarcinoma. *Am. J. Respir. Crit. Care Med. 160:1269.*
57. Giachelli, C. M., D. Lombardi, R. J. Johnson, C. E. Murry, and M. Almeida. 1998. Evidence for a role of osteopontin in macrophage infiltration in response to pathological stimuli in vivo. *Am. J. Pathol. 152:353.*
58. Weber, G. F., S. Ashkar, M. J. Glimcher, and H. Cantor. 1996. Receptor-ligand interaction between CD44 and osteopontin (Eta-1). *Science 271:509.*
59. Asou, Y., S. R. Rittling, H. Yoshitake, K. Tsuji, K. Shinomiya, A. Nifuji, D. T. Denhardt, and M. Noda. 2001. Osteopontin facilitates angiogenesis, accumulation of osteoclasts, and resorption in ectopic bone. *Endocrinology 142:1325.*